



J. Serb. Chem. Soc. 74 (5) 555–571 (2009)
JSCS–3855

Theoretical and experimental investigations on the structure and vibrational spectra of 6-amino-3-methyl-1-phenyl-1*H*-pyrazolo[3,4-*b*]pyridine-5-carboxylic acid and 6,7-dihydro-3-methyl-6-oxo-1-phenyl-1*H*-pyrazolo[3,4-*b*]pyridine-5-carbonitrile

KHALED BAHGAT^{1*}, NAZM AL-DEN JASEM² and TALAAT EL-EMARY³

¹Chemistry Department, Faculty of Petroleum and Mining Engineering, Suez Canal University, Suez, Egypt, ²Chemistry Department, Faculty of Sciences, Aleppo University, Syria and ³Chemistry Department, Faculty of Science, Assiut University, Assiut, Egypt

(Received 22 October 2008, revised 12 February 2009)

Abstract: The solid phase FT-IR and FT-Raman spectra of 6-amino-3-methyl-1-phenyl-1*H*-pyrazolo[3,4-*b*]pyridine-5-carboxylic acid (PYRPCA) and 6,7-dihydro-3-methyl-6-oxo-1-phenyl-1*H*-pyrazolo[3,4-*b*]pyridine-5-carbonitrile (PYRPCN) were recorded in the region 4000–400 cm⁻¹. The spectra were interpreted with the aid of normal coordinate analysis following full structure optimization and force field calculations based on the density functional theory (DFT) using standard B3LYP, BLYP and *ab initio* RHF methods with 6-31G* basis set and were scaled using a recommended set of scaling factors yielding fairly good agreement between the observed and calculated frequencies. Based on the present good quality, the scaled quantum mechanical (SQM) force field, a reliable description of the fundamentals of PYRPCA and PYRPCN, was provided. The calculations predicated a predominance of different tautomers in PYRPCA and keto-enol tautomers in PYRPCN. For PYRPCA, the most stable conformer is stabilized by intramolecular hydrogen bonding. The characteristic of the hydrogen bonding is its strengthening effect on the conjugation of the NH₂ and COOH groups with the pyridine ring.

Keywords: DFT calculations; vibrational spectra; 6-amino-3-methyl-1-phenyl-1*H*-pyrazolo[3,4-*b*]pyridine-5-carboxylic acid; 6,7-dihydro-3-methyl-6-oxo-1-phenyl-1*H*-pyrazolo[3,4-*b*]pyridine-5-carbonitrile.

INTRODUCTION

In the past two decades, quantum chemical computational methods have proven themselves to be essential tools for interpreting and predicting vibrational spectra.^{1,2} A significant advance in this area was made by combining empirical and *ab initio* information in the scaled quantum mechanical (SQM) force field me-

* Corresponding author. E-mail: khabahgat1@hotmail.com
doi: 10.2298/JSC0905555B

thod.³⁻⁷ In the SQM method, the computed harmonic force field is improved usually by a few scale factors, obtained by fitting theoretical vibrational frequencies to experimental data. These scale factors were generally found to be well transferable between chemically related molecules, nibbling to obtain reliable vibrational information for a large variety of organic compounds.⁸⁻¹² For organic molecules containing a hydrogen bonded system, the scaled B3LYP/6-31G* force field, using unscaled factors recommended by Rauhat and Pulay for large scale studies,⁸ also provided a proper description of the vibrational properties of these molecules. However, few publications are devoted to the chemistry of pyrazolo pyridines derivatives.¹³ The UV absorption spectra for several bis-pyrazolopyridine derivatives were provided using the TDDFT method.¹⁴

6-Amino-3-methyl-1-phenyl-1*H*-pyrazolo[3,4-*b*]pyridine-5-carboxylic acid (PYRPCA) and 6,7-dihydro-3-methyl-6-oxo-1-phenyl-1*H*-pyrazolo[3,4-*b*]pyridine-5-carbonitrile (PYRPCN) are interesting representatives of pyrazolo pyridine derivatives. Due to conjugation with the π system of the pyridine ring and a possible intermolecular hydrogen bond formation, the carboxylic group in PYRPCA may play an important role in pyrazolo-pyridine tautomerism. Also, 6,7-dihydro-3-methyl-6-oxo-1-phenyl-1*H*-pyrazolo[3,4-*b*]pyridine-5-carbonitrile (PYRPCN) carrying an NH at the peri position to a carbonyl group is a characteristic representative of keto-enol forms with a strong HB.

The aim of the present study was to determine the structure (tautomerism and hydrogen bonding) and subsistent effect on the vibrational spectra of 6-amino-3-methyl-1-phenyl-1*H*-pyrazolo[3,4-*b*]pyridine-5-carboxylic acid (PYRPCA) and 6,7-dihydro-3-methyl-6-oxo-1-phenyl-1*H*-pyrazolo[3,4-*b*]pyridine-5-carbonitrile (PYRPCN) by the concentrated application of quantum chemical calculations and vibrational spectroscopy. Based on experimental FT-IR and FT-Raman data, a complete vibrational analysis of the molecules was performed using the Pulay DFT-based SQM method.⁴ The ground state geometries were optimized using DFT with B3LYP and BLYP and *ab initio* restricted Hartree-Fock methods with the 6-31G* basis set, and comparing the effect of simpler and more elaborate versions of scaling, while paying attention to ensuring correct band assignment. The calculated infrared and Raman spectra of the title compounds were simulated utilizing the computed dipole derivatives for IR intensities and polarizability derivatives for Raman intensities.

EXPERIMENTAL

6-Amino-3-methyl-1-phenyl-1*H*-pyrazolo[3,4-*b*]pyridine-5-carboxylic acid and 6,7-dihydro-3-methyl-6-oxo-1-phenyl-1*H*-pyrazolo[3,4-*b*]pyridine-5-carbonitrile were obtained as previously described in the literature.^{15,16}

The infrared spectra were recorded with a Nicolet Magna 750 FT-IR spectrometer equipped with a room temperature DTGS detector. The spectra of the solid (in the 4000–400 cm^{-1} spectral region) were recorded in the form of KBr pellets at a 2 cm^{-1} spectral resolution accumulating 128 scans.

The Raman spectra were measured with a Nicolet 950 FT-Raman spectrometer equipped with a liquid nitrogen cooled Ge detector. An Nd:YAG laser (1064 nm) was used for excitation at 30–150 mW output power at a spectral resolution of 4 cm⁻¹.

Computational details

The molecular geometry optimization, energy and vibrational frequency calculations were performed with the GAUSSIAN 94W software package,¹⁷ using the B3LYP functionals BLYP and RHF,^{18,19} combined with the standard 6-31G* basis set. The cartesian representation of the theoretical force constants were computed at the optimized geometry by assuming C1 point group symmetry. Scaling of the force field was performed according to the SQM procedure,^{4,8} using selective scaling in the natural internal coordinate representation.^{5,20} Transformations of the force field and subsequent normal coordinate analysis, including the least square refinement of the scaling factors, calculation of potential energy distribution (PED) and the prediction of IR and Raman intensities, were realized on a PC with the MOLVIB program (version 7.0 – G77) written by Sundius.²¹⁻²³ For the plots of the simulated IR and Raman spectra, pure Lorentzian band shapes were used with a bandwidth (FWHM) of 6 cm⁻¹. The symmetry of the molecules was also helpful in making the vibrational assignments. The symmetries of the vibrational modes were realized using the standard procedure.²⁴ The symmetry analysis for the vibrational modes of the title molecules are presented in some detail in order to describe the basis for the assignments.

RESULTS AND DISCUSSION

Tautomerization and conformation

The molecular structures of PYRPCA and PYRPCN are shown in Figs. 1 and 2, respectively. The bond lengths and bond angles determined at the DFT level of the theory for the title compounds are listed in Table I. The global minimum energy obtained by DFT structure optimization for the title compound is presented in Table II. The geometrical optimization studies of PYRPCA and PYRPCN revealed that the molecules belong to the C1 symmetry point group, in which the phenyl ring make a dihedral angle of 26.23° with the adjacent pyrazole ring. The conformational variation of PYRPCA compound involve four tautomers/conformers, due to the different substitution in position 8 and 7 of the pyridine ring (numbering as in Fig. 1), and conformational variation, evolving from H-proton transfer and the relative orientation of the amino and carbonyl groups. PYRPCN involves three tautomers, in which conformational variation evolves from keto–enol tautomerization, and constitutes an intriguing set of compounds that form strong intra-molecular hydrogen bonds. The energies for the possible tautomers/conformers of the title compounds were calculated at the 6-31G* basis sets and they are listed in Table II. The energy obtained for **Ia** and **Ib** tautomers of the studied compounds at B3LYP, BLYP and RHF at 6-31G* bases set were found to be the global minimum. The large stability of the conformers **Ia** results from a shortening of the O14···H11 (1.935 Å) contact with respect to the **IIa** conformer (2.547 Å), as well as to its non-hydrogen-bonded counterpart.

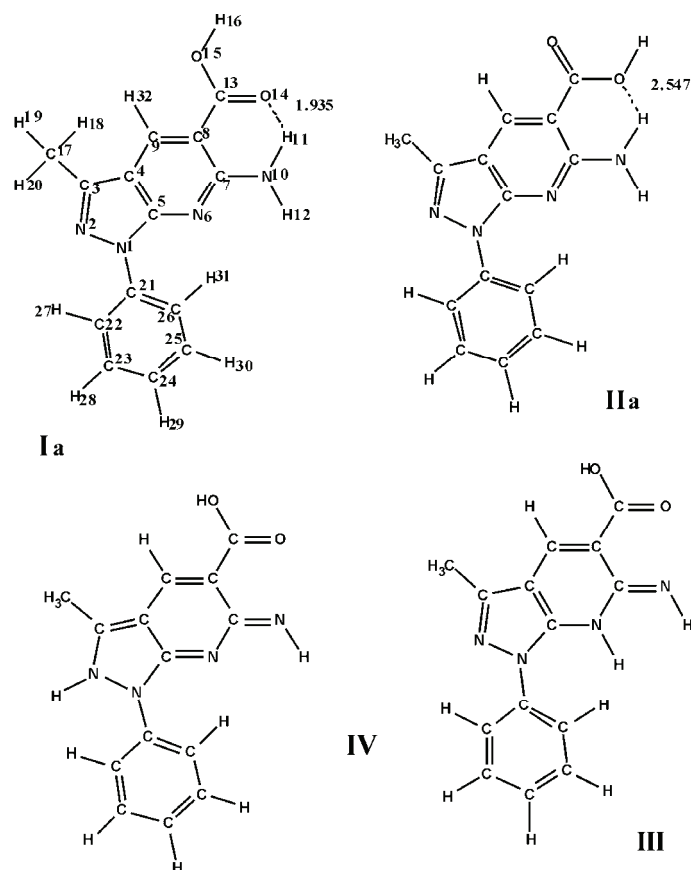


Fig. 1. The conformers considered and the numbering of the atoms in the PYRPCA molecule.

Geometric structure and hydrogen bonding

Structural analysis revealed the presence of intramolecular hydrogen bond interactions in PYRPCA and intermolecular hydrogen bond in PYRPCN. The $\text{CO}\cdots\text{NH}$ hydrogen bond in the **Ia** tautomer of PYRPCA and the $\text{N-H}\cdots\text{O}$ hydrogen bond in the **Ib** tautomer of PYRPCN are very similar in their characteristics to analogous compounds,^{25–27} in which NH_2 , NH and C=O groups participate in several inter-molecular and intra-molecular hydrogen bonds.^{28–31} The strength of the interactions can be related to the length of the hydrogen bond. The shorter $\text{O}\cdots\text{H}$ contact is in agreement with the large stability of **Ia** with respect to the non-hydrogen-bonded counterpart (*cf.* Figs. 1 and 2). The strength of hydrogen bond is also supported by the geometrical characteristics, most significant of which are the large elongation of C13-O14 and N10-H11 (in PYRPCA) and the large tilt of the NH_2 group towards the carbonyl group and rotation by 90° of the COOH group as compared to the other non-hydrogen-bonded isomers. Moreover,

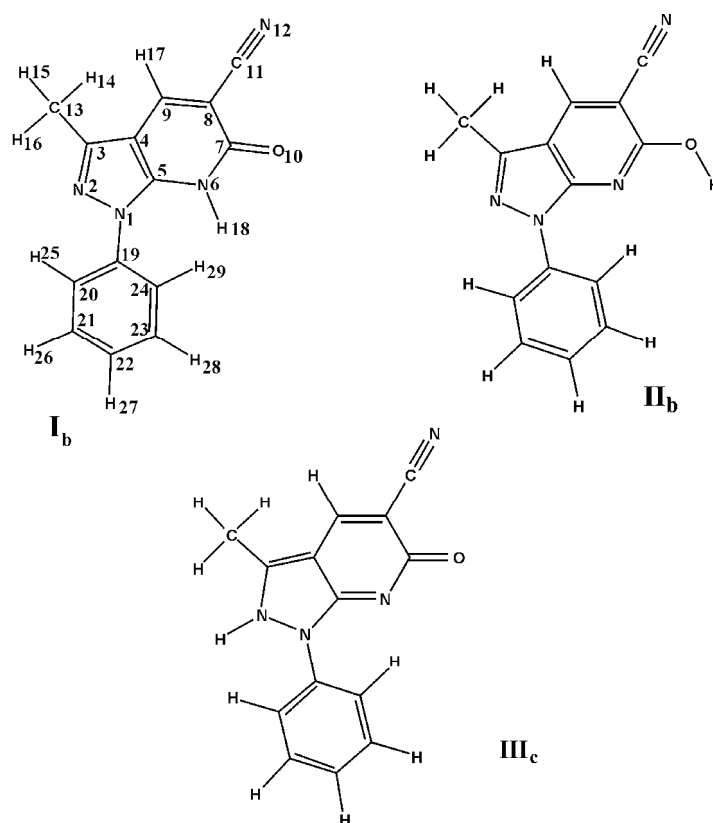


Fig. 2. The conformers considered and the numbering of the atoms of the PYRPCN molecule.

the computed C13–O14 and N10–H11 bond lengths in PYRPCA are too large compared with similar compounds.²⁵ Also, the computed C8–C13 and C7–N10 bond distances seem to be somewhat short. These geometrical parameters are sensitive to hydrogen bonding.²⁶ The hydrogen bonding interaction in **I_a** has a strong promoting effect on the conjugation of the NH₂ and COOH groups with the pyridine ring. A strengthening of the double bond character of C7–N10 and C8–C13 is indicated by a shortening of these bonds by 0.12 and 0.03 Å, respectively (*cf.* Table I). The intra-molecular hydrogen bond in PYRPCN affects the N–H and C=O bond lengths; thus in the case of the **I_b** tautomer, this lengthening amounts to 0.09 Å for the N–H and 0.04 Å for the C=O bonds, compared with similar compounds.²⁷ These changes are in agreement with the resonance character of this tautomeric system.

Vibrational spectra

The PYRPCA and PYRPCN molecules are not planar, with the phenyl ring making a dihedral angle of 26.230° with the adjacent pyrazole ring. As a result of

TABLE I. Optimized geometrical parameters of PYRPCA and PYRPCN (values for PYRPCN in parentheses); for the numbering of the atoms, see Figs. 1 and 2

Bond	Bond length, Å			Bond	Bond angle, deg.		
	B3LYP	BLYP	RHF		B3LYP	BLYP	RHF
N1-C2	1.388 (1.391)	1.408 (1.413)	1.374 (1.373)	N1-C2-C3	107.667 (106.420)	107.170 (106.040)	108.340 (106.990)
N2-C3	1.313 (1.332)	1.330 (1.330)	1.280 (1.290)	N2-C3-C4	110.437 (110.980)	110.720 (111.460)	110.060 (110.560)
C3-C4	1.433 (1.434)	1.440 (1.440)	1.430 (1.430)	C3-C4-C5	105.170 (104.240)	105.480 (104.350)	104.920 (103.750)
C4-C5	1.420 (1.380)	1.430 (1.410)	1.400 (1.370)	C4-C5-N6	126.014 (122.740)	126.150 (121.900)	125.760 (122.670)
C5-N6	1.333 (1.360)	1.340 (1.370)	1.320 (1.350)	C5-N6-C7	116.095 (122.750)	115.870 (122.900)	116.640 (122.290)
N6-C7	1.344 (1.410)	1.350 (1.430)	1.320 (1.390)	N6-C7-C8	122.965 (114.220)	123.150 (114.130)	122.780 (114.710)
C7-C8	1.449 (1.435)	1.460 (1.480)	1.440 (1.470)	C7-C8-C9	118.577 (122.400)	118.460 (122.430)	118.250 (122.110)
C8-C9	1.396 (1.380)	1.340 (1.390)	1.380 (1.350)	N10-C7-N6	116.332 (119.760)	116.210 (110.970)	115.820 (119.710)
N10-C7	1.350	1.360	1.330	C8-C7-N10	120.704	120.530	121.280
N10-H11	1.012	1.020	0.990	C7-N10-H11	119.439	118.930	121.050
N10-H12	1.008	1.010	0.990	C7-N10-H12	118.180	118.270	117.900
C13-C8	1.466	1.470	1.460	C7-C8-C13	120.678	120.560	121.310
C13-O14	1.227	1.240	1.190	C8-C13-O14	126.243	126.243	126.180
C13-O15	1.359	1.370	1.330	C8-C13-O15	113.491	113.470	113.380
O15-H16	0.974	0.980	0.950	C13-O15-H16	105.349	104.420	107.450
O14-H11	1.935	1.930	2.006	N2-C3-C17	121.008	120.490	121.690
C17-C3	1.496	1.500	1.490	N2-N1-C21	118.621	118.560	118.470
C17-H18	1.093	1.010	1.080	C24-C25-C26	121.027	121.040	121.100
C17-H19	1.097	1.010	1.080	N2-N1-C21-C22	26.32	26.41	26.89
C17-H20	1.097	1.010	1.080	N10-C7-N6-C5	179.84	179.980	180.00
C21-N1	1.421	1.430	1.410	O14-C13-C8-C9	179.48	179.960	179.980
C22-C21	1.403	1.410	1.390	O15-C13-C8-C7	179.97	179.960	179.970
C23-C22	1.392	1.400	1.380	N6-C7-O10	(119.710)	(119.400)	(119.880)
C24-C23	1.396	1.400	1.380	C7-C8-C11	(109.85)	(110.880)	(110.180)
C25-C24	1.395	1.400	1.380	N2-N1-C19-C20	(37.880)	(36.290)	(38.910)
C26-C25	1.381	1.400	1.380	N2-N1-C19-C24	(141.757)	(143.240)	(143.870)

the C1 symmetry, the 90 and 81 fundamentals for PYRPCA and PYRPCN, respectively, are active in both the infrared absorption and Raman scattering. The FT-IR and FT-Raman spectra of PYRPCA and PYRPCN molecules are shown in Figs. 3–6, respectively. The absence of definite bands in the OH stretching region of the experimental IR and Raman spectra of PYRPCN suggests that no enol tautomer is present in the solid phase of the PYRPCN molecule. The absence of this

TABLE II. Total energies (in hartrees) of PYRPCA obtained from B3LYP/6-31G* calculations

Conformers	PYRPCA	PYRPCN
I	-910.206137 ^a	-833.7311
II	-910.166388	-833.6541
III	-910.150738	-833.7132
IV	-910.111532	

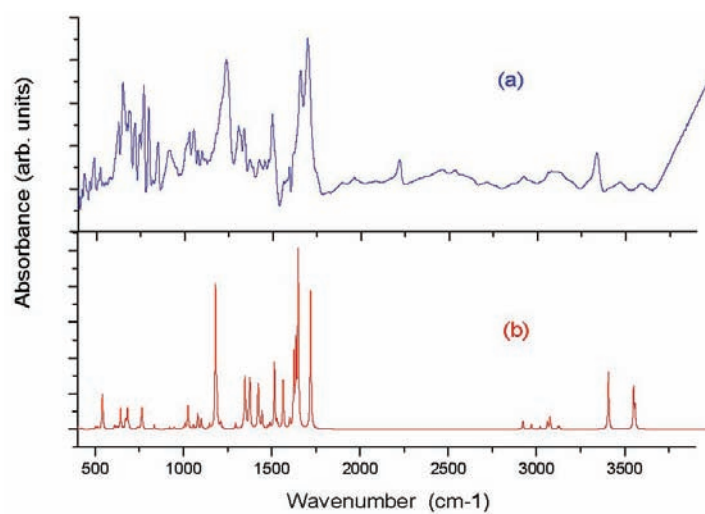
^aGlobal minimum energy

Fig. 3. FT-IR spectra of PYRPCA; a) observed, b) calculated.

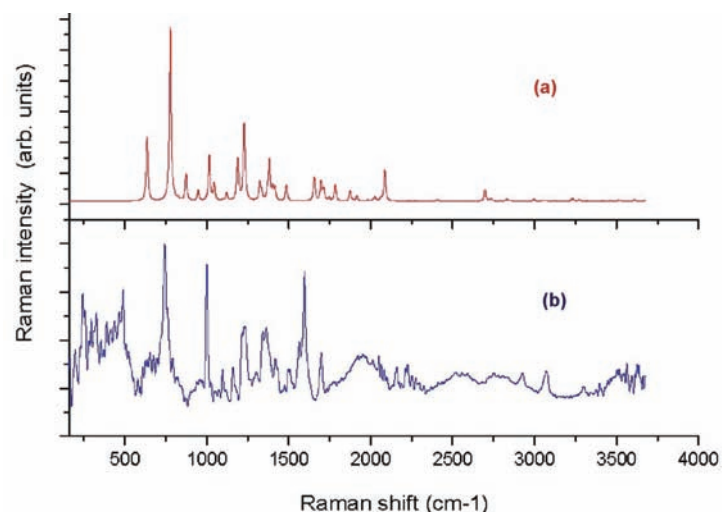


Fig. 4. FT-Raman spectra of PYRPCA; a) calculated, b) observed.

band is a general spectral feature of enolized β -diketones, attributed to the electron configuration of the chelate ring.²⁸ The results of the present vibrational analysis, *viz.*, calculated unscaled vibrational frequencies, IR and Raman intensities, SQM frequencies; potential energy distribution (PED) and assignment of the fundamentals, are shown in Table V-SM (Supplementary material). The well-known good performance of the density functional theory for the estimation of the vibrational spectra of organic compounds can be observed also in case of the **Ia** and **Ib** conformer. The interpretation of the experimental spectra was based on the scaled computed B3LYP/6-31G* force field utilizing additional information from computed (unscaled) IR intensities and Raman activities. The choice of the B3LYP force field was reasoned by the found good agreement between the B3LYP results for the HB interaction and geometrical parameters of the **Ia** and **Ib** conformers. In fact, a rough assignment can already be performed based on the unscaled computed results. However, for reliable information on the vibrational properties (e.g., good quality force field), the use of selective scaling is necessary.

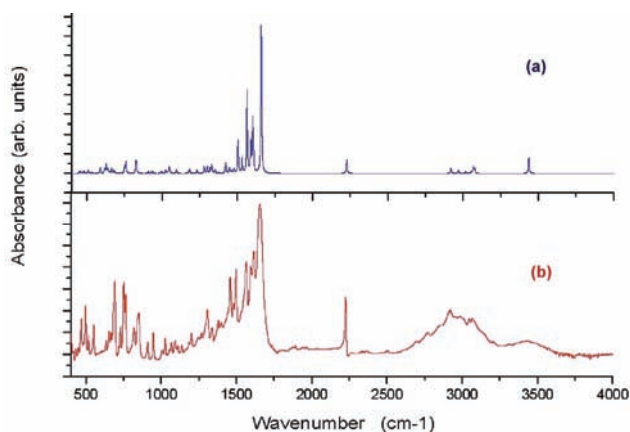


Fig. 5. FT-IR spectra of PYRPCN; a) calculated, b) observed.

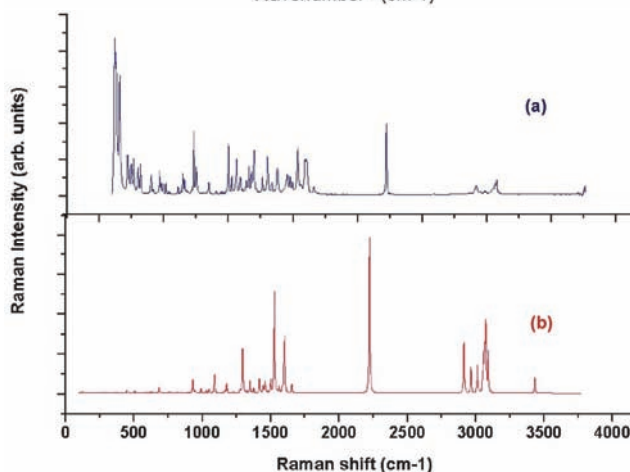


Fig. 6. FT-Raman spectra of PYRPCN; a) observed, b) calculated.

SQM analysis, assignment

The effect of scaling was studied using the DFT force fields of the title compounds. Several calculations were performed with different kinds of scaling. Calculations A performed with the unscaled (raw) DFT force field transformed to the natural internal coordinates; calculation B, labeled C_0 , was performed with selective scaling according to the SQM scheme, using 9 transferable scale factors from the recommended set⁴ without refinement. In calculation of C_{ref} , the number of distinct scale factors was increased to 15 (as shown in the last columns of Tables III and IV) and 14 of these were refined in a least-squares procedure to achieve a better frequency fit. Special attention was paid to the vibrations of the OH, NH₂, NH and C=O groups, whether the errors of the B3LYP/6-31G* level for hydrogen bonding were not sufficiently corrected by the original scale factors. This SQM treatment resulted in a weighted mean deviation of 81.81 cm⁻¹ for PYRPCA and 73.21 cm⁻¹ for PYRPCN. The largest deviations between the experimental and SQM frequencies were observed for the vibration of the NH₂, OH, NH and CO groups. The following were registered:

- OH stretch, an overestimation of *ca.* 114 cm⁻¹;
- NH stretch, an overestimation of *ca.* 158 cm⁻¹;
- CN stretch, an overestimation of *ca.* 121 cm⁻¹;
- NH₂ stretch, an overestimation of *ca.* 152 cm⁻¹;
- C=O stretch, an overestimation of 80 cm⁻¹ by the scaled B3LYP/6-31G* force field.

TABLE III. Definition of the local symmetry coordinates for 6-amino-3-methyl-1-phenyl-1*H*-pyrazolo[3,4-*b*]pyridine-5-carboxylic acid and the values of the corresponding scale factors used to correct the B3LYP/6-31G* (C_0 , C_{ref}) force fields

No(i)	Symbol	Definition	Scale factors used		
			Notat	C_0	C_{ref}
1-6	CHar	$R_1, R_2, R_3, R_4, R_5, R_6$	S1-S6	0.920	0.931
7	CH ₃ ss	$(R_7+R_8+R_9)/\sqrt{3}$	S7	0.920	0.920
8	CH ₃ ips	$(2R_7-R_8-R_9)/\sqrt{6}$	S8	0.920	0.920
9	CH ₃ ops	$(R_8-R_9)/\sqrt{2}$	S9	0.920	0.920
10	CCH ₃	T ₁₀	S10	0.922	0.922
11-15	CN	$q_{11}, q_{12}, q_{13}, q_{14}, q_{15}$	S11-S15	0.922	0.922
16-26	CCar	$R_{16}, R_{17}, R_{18}, R_{19}, R_{20}, R_{21}, R_{22}, R_{23}, R_{24}, R_{25}, R_{26}$	S16-S26	0.922	0.984
27	NN	P ₂₇	S27	0.922	0.922
28	CNH ₂	P ₂₈	S28	0.922	0.922
29-30	NH ₂	P_{29}, P_{30}	S29-S30	0.922	0.965
31	CCO ₂	P ₃₁	S31	0.922	0.984
32-33	CO ₂	P_{32}, P_{33}	S32-S33	0.922	0.896
34	OH	P ₃₄	S34	0.920	0.920
35-40	bCH _{ar}	$(\alpha_{35}-\alpha_{36})/\sqrt{2}, (\alpha_{37}-\alpha_{38})/\sqrt{2}, (\alpha_{39}-\alpha_{40})/\sqrt{2}$ $(\alpha_{41}-\alpha_{42})/\sqrt{2}, (\alpha_{43}-\alpha_{44})/\sqrt{2}, (\alpha_{45}-\alpha_{46})/\sqrt{2}$	S35-S40	0.950	0.950

TABLE III. Continued

No(i)	Symbol	Definition	Scale factors used		
			Notat	C ₀	C _{ref}
41	CH ₃ sb	$(-\alpha_{47}-\alpha_{48}-\alpha_{49}+\beta_{50}+\beta_{51}+\beta_{52})/\sqrt{6}$	S41	0.915	0.915
42	CH ₃ ipb	$(-\beta_{50}-\beta_{51}+2\beta_{52})/\sqrt{6}$	S42	0.915	0.915
43	CH ₃ opb	$(-\beta_{50}-\beta_{51})/\sqrt{2}$	S43	0.915	0.915
44	CCH ₃	$(\alpha_{53}-\alpha_{54})/\sqrt{2}$	S44	0.950	0.950
45	bR1	$\beta_{55}+a(\beta_{56}+\beta_{58})+b(\beta_{57}+\beta_{59})$	S45	0.990	0.990
46	bR1	$(a-b)(\beta_{56}-\beta_{58})+(1-a)(\beta_{57}+\beta_{59})$	S46	0.990	0.990
47	R2trigd	$(\alpha_{60}-\alpha_{61}+\alpha_{62}-\alpha_{63}+\alpha_{64}-\alpha_{65})/\sqrt{6}$	S47	0.990	0.990
48	R2sym	$(-\alpha_{60}-\alpha_{61}+2\alpha_{62}-\alpha_{63}-\alpha_{64}+2\alpha_{65})/\sqrt{12}$	S48	0.990	0.990
49	R2asym	$(\alpha_{60}-\alpha_{61}+2\alpha_{63}+\alpha_{64})/2$	S49	0.990	0.990
50	bCNH ₂	$(\delta_{66}-\delta_{67})/\sqrt{2}$	S50	0.950	0.950
51	bNH ₂	$(\delta_{68}-\delta_{69})/\sqrt{2}$	S51	0.915	0.915
52	bNH ₂	$(2\delta_{70}-\delta_{68}-\delta_{69})/\sqrt{6}$	S52	0.915	0.915
53	bCCO ₂	$(\delta_{71}-\delta_{72})/\sqrt{2}$	S53	0.99	0.99
54	bCO ₂	$(\delta_{73}-\delta_{74})/\sqrt{2}$	S54	0.990	0.876
55	bCO ₂	$(2\sigma_{75}-\sigma_{73}-\sigma_{74})/\sqrt{6}$	S55	0.990	0.876
56	bOH	δ_{76}	S56	0.990	0.990
57-58	bCN1	$(\theta_{77}-\theta_{78})/\sqrt{2}, (\theta_{79}-\theta_{80})/\sqrt{2}$	S57-S58	0.990	0.990
59	R3trigd	$(\alpha_{81}-\alpha_{82}+\alpha_{83}-\alpha_{84}+\alpha_{85}-\alpha_{86})/\sqrt{6}$	S59	0.990	0.990
60	R3sym	$(-\alpha_{81}-\alpha_{82}+2\alpha_{83}-\alpha_{84}-\alpha_{85}+2\alpha_{86})/\sqrt{12}$	S60	0.990	0.990
61	R3asym	$(\alpha_{81}-\alpha_{82}+2\alpha_{84}+\alpha_{85})/2$	S61	0.990	0.990
62-67	gCH _{ar}	$\omega_{87}, \omega_{88}, \omega_{89}, \omega_{90}, \omega_{91}, \omega_{92}$	S62-S67	0.976	0.976
68-69	gCC _{ar}	ω_{93}, ω_{94}	S68-S69	0.976	0.976
70	gCCO ₂	ω_{95}	S70	0.976	0.976
71-72	gCN1	ω_{96}, ω_{97}	S71-S72	0.976	0.976
73	gCNH ₂	ω_{98}	S73	0.976	0.976
74	gNH ₂	ω_{99}	S74	0.806	0.806
75	gCCH ₃	ω_{100}	S75	0.976	0.984
76	gCO ₂	ω_{101}	S76	0.976	0.976
77	tR1	$\tau_{102}+b(\tau_{103}+\tau_{105})+a(\tau_{104}-\tau_{106})$	S77	0.935	0.935
78	tR1	$(a-b)(\tau_{103}-\tau_{105})+(1-a)(\tau_{104}-\tau_{106})$	S78	0.935	0.935
79	tR2trigd	$(\tau_{107}+\tau_{108}+\tau_{109}+\tau_{110}+\tau_{111}+\tau_{112})/\sqrt{6}$	S79	0.935	0.935
80	tR2sym	$(\tau_{107}+\tau_{108}+\tau_{110}+\tau_{111})/\sqrt{2}$	S80	0.935	0.935
81	tR2asym	$(-\tau_{107}+\tau_{108}+2\tau_{109}-\tau_{110}-\tau_{111}+2\tau_{112})/\sqrt{12}$	S81	0.935	0.935
82					
83	tR3trigd	$(\tau_{113}+\tau_{114}+\tau_{116}+\tau_{117})/\sqrt{2}$	S82	0.935	0.935
84	tR3sym	$(\tau_{113}+\tau_{114}+\tau_{116}+\tau_{117})/\sqrt{2}$	S83	0.935	0.935
85	tR3asym	$(-\tau_{113}+\tau_{114}+2\tau_{115}-\tau_{116}-\tau_{117}+2\tau_{118})/\sqrt{12}$	S84	0.935	0.935
86					
87	tCH ₃	τ_{119}	S85	0.831	0.831
88	tCCO ₂	τ_{120}	S86	0.831	0.678
89	tCNH ₂	τ_{121}	S87	0.913	0.910
90	tCN1	τ_{122}	S88	0.831	0.831
	tCO ₂	τ_{123}	S89	0.831	0.831
	Butterfly	τ_{124}	S90	0.913	0.913

In the second step of the SQM analysis, the scale factors for selected vibrations: C=O, NH₂, OH stretch, COH bend, CO wag, OH and ring torsion, were released and optimized using the experimental data. Comparing the experimental and the newly obtained scaled frequencies, some additional systematic deviations could be observed which were smoothed before due to the coupling between the internal coordinates. These were: an overestimation for C=O, NH₂, and CC–O bond. Satisfactory agreement was obtained for C=O and NH stretching in PYRPCN. The final SQM force field (see the column headed C_{ref} in Tables IV and V-SM) reproduced the experimental spectra with a weight mean deviation of 13.9 cm⁻¹ for PYRPCA and 10.12 cm⁻¹ for PYRPCN between the experimental and the scale frequencies. The frequencies of ν_1 , ν_2 , ν_3 and ν_{12} in PYRPCA were excluded from this comparison because of the obvious large effect of intermolecular hydrogen bonding in the solid phase.

TABLE IV. Definition of the local symmetry coordinates for 6,7-dihydro-3-methyl-6-oxo-1-phenyl-1*H*-pyrazolo[3,4-*b*]pyridine-5-carbonitrile (PYRPCN) and the values of the corresponding scale factors used to correct the B3LYP/6-31G* (C₀, C_{ref}) force fields

No(i)	Symbol	Definition	Scale factors used		
			Notat	C ₀	C _{ref}
1	N1H	R ₁	s ₁	0.920	0.914
2–7	CH _{ar}	R ₂ , r ₃ , r ₄ , r ₅ , r ₆ , r ₇	s ₂ → s ₇	0.920	0.914
8	CH _{3ss}	(r ₈ + r ₉ + r ₁₀)/√6	s ₈	0.920	0.914
9	CH _{3ips}	(2r ₈ – r ₉ – r ₁₀)/√6	s ₉	0.920	0.914
10	CH _{3ops}	(r ₉ – r ₁₀)/√2	s ₁₀	0.922	0.922
11	CCH ₃	T ₁₁	s ₁₁	0.922	0.922
12–16	CN	Q ₁₂ , Q ₁₃ , Q ₁₄ , Q ₁₅ , Q ₁₆	s ₁₂ → s ₁₆	0.922	0.926
17–27	CC _{ar}	R ₁₇ , R ₁₈ , R ₁₉ , R ₂₀ , R ₂₁ , R ₂₂ , R ₂₃ , R ₂₄ , R ₂₅ , R ₂₆ , R ₂₇	s ₁₇ → s ₂₇	0.922	0.922
28	NN	P ₂₈	s ₂₈	0.920	0.920
29	C=O	P ₂₉	s ₂₉	0.922	0.830
30	CC(N)	P ₃₀	s ₃₀	0.922	0.922
31	C≡N	P ₃₁	s ₃₁	0.922	0.897
32–37	bCH _{ar}	(α ₃₂ – α ₃₃)/√2, (α ₃₄ – α ₃₅)/√2, (α ₃₆ – α ₄₇)/√2	s ₃₂ → s ₃₇	0.950	0.950
38	CH _{3sb}	(α ₃₈ – α ₃₉)/√2, (α ₄₀ – α ₄₁)/√2, (α ₄₂ – α ₄₃)/√2	s ₃₈	0.950	0.950
39	CH _{3ipb}	(–α ₄₄ – α ₄₅ – α ₄₆ + β ₄₇ + β ₄₈ + β ₄₉)/√6	s ₃₉	0.915	0.915
40	CH _{3opb}	(–β ₄₇ – β ₄₈ + 2β ₄₉)/√6	s ₄₀	0.915	0.915
41	CH _{3ipr}	(β ₄₇ – β ₄₈)/√2	s ₄₁	0.915	0.915
42	CH _{3opr}	(2α ₄₄ – α ₄₅ – α ₄₆)/√6	s ₄₂	0.915	0.915
43	bR1	(α ₅₀ – α ₅₁)/√2	s ₄₃	0.915	0.915
44	bR1	β ₅₂ + a(β ₅₃ + β ₅₅) + b(β ₅₄ + β ₅₆)	s ₄₄	0.990	0.990
45	R2trigd	(a – b)(β ₅₃ – β ₅₅) + (1 – a)(β ₅₄ – β ₅₆)	s ₄₅	0.990	0.990
46	R2sym	(α ₅₇ – α ₅₈ + α ₅₉ – α ₆₀ + α ₆₁ – α ₆₂)/√6	s ₄₆	0.990	0.990
47	R2asym	(–α ₅₇ – α ₅₈ + 2α ₅₉ – α ₆₀ – α ₆₁ + 2α ₆₂)/√12	s ₄₇	0.990	0.990
48	bC=O	(α ₅₇ – α ₅₈ + α ₆₀ – α ₆₁)/2	s ₄₈	0.990	0.990
49	bN1H	(δ ₆₃ – δ ₆₄)/√2	s ₄₉	0.950	0.913
50	bCC(N)	(δ ₆₅ – δ ₆₆)/√2	s ₅₀	0.950	0.915

TABLE IV. Continued

No(i)	Symbol	Definition	Scale factors used		
			Notat	C ₀	C _{ref}
51	bC≡N _{in}	$(\delta_{66} - \delta_{68})/\sqrt{2}$	S ₅₁	0.915	0.950
52–53	bC≡N _{op}	δ_{69}	S ₅₂ → S ₅₃	0.915	0.913
54	bCN1	δ_{70}	S ₅₄	0.915	0.913
55	R3trigd	$(\theta_{71} - \theta_{72})/\sqrt{2}, (\theta_{73} - \theta_{74})/\sqrt{2}$	S ₅₅	0.915	0.913
56	R3sym	$(\alpha_{75} - \alpha_{76} + \alpha_{77} - \alpha_{78} + \alpha_{79} - \alpha_{80})/\sqrt{6}$	S ₅₆	0.990	0.990
57–62	R3asym	$(-\alpha_{75} - \alpha_{76} + 2\alpha_{77} - \alpha_{78} - \alpha_{79} + 2\alpha_{80})/\sqrt{12}$	S ₅₇ → S ₆₂	0.990	0.990
63–64	gCH _{ar}	$(\alpha_{75} - \alpha_{76} + \alpha_{78} - \alpha_{79})/2$	S ₆₃ → S ₆₄	0.990	0.990
65	gCC _{ar}	$\omega_{81}, \omega_{82}, \omega_{83}, \omega_{84}, \omega_{85}, \omega_{86}$	S ₆₅	0.990	0.934
66–67	gC=O	ω_{87}, ω_{88}	S ₆₆ → S ₆₇	0.976	0.934
68	gCN1	ω_{89}	S ₆₈	0.976	0.976
69	gCC(N)	ω_{90}, ω_{91}	S ₆₉	0.976	0.976
70	gN1H	ω_{92}	S ₇₀	0.976	0.934
71	tR1	ω_{93}	S ₇₁	0.976	0.976
72	tR1	$\tau_{95} + b(\tau_{96} + \tau_{98}) + a(\tau_{97} - \tau_{99})$	S ₇₂	0.831	0.831
73	tR2trigd	$(a - b)(\tau_{96} - \tau_{98}) + (1 - a)(\tau_{97} - \tau_{99})$	S ₇₃	0.831	0.831
74	tR2sym	$(\tau_{100} + \tau_{101} + \tau_{102} + \tau_{103} + \tau_{104} + \tau_{105})/\sqrt{6}$	S ₇₄	0.831	0.831
75	tR2asym	$(\tau_{100} + \tau_{101} + \tau_{103} + \tau_{104})/2$	S ₇₅	0.831	0.831
76	tR3trigd	$(-\tau_{100} - \tau_{103} + 2\tau_{102} - \tau_{103} - \tau_{104} + 2\tau_{105})/\sqrt{12}$	S ₇₆	0.831	0.831
77	tR3sym	$(\tau_{106} + \tau_{107} + \tau_{108} + \tau_{109} + \tau_{110} + \tau_{111})/\sqrt{6}$	S ₇₇	0.831	0.831
78	tR3asym	$(\tau_{106} + \tau_{107} + \tau_{109} + \tau_{110})/2$	S ₇₈	0.831	0.831
79	tCH ₃	$(-\tau_{106} - \tau_{107} + 2\tau_{108} - \tau_{109} - \tau_{110} + 2\tau_{111})/\sqrt{12}$	S ₇₉	0.831	0.831
80	tC19N	τ_{112}	S ₈₀	0.831	0.831
81	Butterfly	τ_{113}	S ₈₁	0.831	0.935
		τ_{114}		0.935	0.935

COOH vibrations

Hydrogen bonding alters the frequencies of the stretching and bending vibrations. The O–H stretching bands move to lower frequencies, usually with increased intensity and band broadening in hydrogen bonded species. In the present study, the O–H stretching frequency was observed at 3407 cm⁻¹.²⁸ However, the wave number calculated by the B3LYP method showed a strong negative deviation of 214 cm⁻¹. The C–O stretching is a characteristic frequency of carboxylic acid.²⁹ The strong band appearing at 1697 cm⁻¹ in the FT-IR spectrum was assigned as the C=O stretching vibration. The theoretical value of 1721 cm⁻¹ computed by the B3LYP method showed a negative deviation of 24 cm⁻¹ because of mixing with the pyridine ring vibrations.^{30,32} The O–H in-plane bending occurred between 1440 and 1395 cm⁻¹ and the out-of-plane bending vibration at between 970 and 875 cm⁻¹.³³ The medium band at 1419 cm⁻¹ in FT-IR spectrum was assigned as the O–H in-plane bending vibration and frequency at 935 cm⁻¹ to the O–H out-of-plane bending vibration for the present molecule. The theoretically computed value of 1382 cm⁻¹ is in very good agreement for the O–H in-plane bending vibration. However, the calculated value of OH out-of-pla-

ne bending deviates positively by about 200 cm^{-1} . This shift in the O–H out-of-plane bending vibration reflects on the strength of the hydrogen bond. The band observed at 1186 cm^{-1} in FT-Raman spectrum of PYRPCA corresponds to the C–COOH stretching vibration. The calculated result at 1182 cm^{-1} is in excellent agreement with the experimental data.

C≡N vibrations

The assignment of the highly characteristic nitrile stretching mode ($\nu(\text{C}\equiv\text{N})$) to the band at 2224 cm^{-1} is quite obvious in all calculations. The degenerate pair of linear bending vibrations of the C–C≡N moiety is split into in-plane and out-of-plane components, both strongly mixed with several other in-plane and out-of-plane vibrations, respectively. They contribute to several normal modes in the $600\text{--}100\text{ cm}^{-1}$ range (see Table V-SM). In the final force field, the in-plane linear bend has a smaller force constant (0.319 N/cm) than the out-of-plane counterpart (0.399 N/cm), which may be due to a stronger interaction of the latter with the p-electrons of the pyridine ring.

Amino group vibrations

The frequencies of the amino group appear at around $3500\text{--}3300\text{ cm}^{-1}$ for the N–H stretching, $1700\text{--}1600\text{ cm}^{-1}$ for the scissoring and $1150\text{--}900\text{ cm}^{-1}$ for the rocking deformations.³⁴ In the present study, the NH_2 asymmetric and symmetric stretching modes move to lower frequencies, usually with increased intensity and band broadening in the hydrogen bonded species. The FT-IR bands at 3407 and 3301 cm^{-1} in the infrared spectrum and at 3413 and 3311 cm^{-1} in the Raman spectrum of PYRPCA were assigned to NH_2 asymmetric and symmetric stretching, respectively. The bands observed at 1597 cm^{-1} in the infrared and Raman are assigned undoubtedly to the scissoring modes of the NH_2 group. According to PED, this band is strongly mixed with the NH_2 rocking mode. According to NCA calculations, the medium and weak IR bands at 1027 and 796 cm^{-1} are assigned to NH_2 rocking and NH_2 out-of-plane bending, respectively.

Methyl group vibrations

For the assignments of CH_3 group frequencies, basically nine fundamentals can be associated to each CH_3 group, namely: CH_3 ss, symmetrical stretch; CH_3 ips, in-plane stretch (*i.e.*, in-plane hydrogen stretching modes); CH_3 ipb, in-plane-bending (*i.e.*, hydrogen deformation modes); CH_3 sb, symmetric bending; CH_3 ipr, in-plane rocking; CH_3 opr, out-of-plane rocking and CH_3 t, twisting hydrogen bending modes, as well as, CH_3 ops, out-of-plane stretch and CH_3 opb, out-of-plane bending modes of the CH_3 group. For PYRPCA, the CH_3 ss frequency was established at 2921 cm^{-1} in the IR spectrum of both compounds and CH_3 ips was found at 3045 and 3042 cm^{-1} in the IR and Raman, respectively. These bands were also observed at 3022 and 3017 cm^{-1} in the IR and Raman

spectrum, respectively, of PYRPYCN. These assignments are also supported by the literature.³⁵ The two in-plane methyl hydrogen deformation modes are also well established. The symmetrical methyl deformation was observed at 1354 and 1356 cm^{-1} in the infrared and Raman spectrum of PYRPCA, and the in-plane-bending methyl deformation mode at 1455 cm^{-1} in the Raman spectrum. These bands were observed at 1378 and 1381 cm^{-1} in the infrared and Raman spectrum of PYRPCN and at 1446 cm^{-1} for the methyl in-plane-bending. The bands at 3027 and 1432 cm^{-1} in the infrared spectrum of PYRPCA were attributed to CH_3 ops and CH_3 opb, respectively. These bands were observed at 3047 and 1455 cm^{-1} in the infrared spectrum of PYRPCN. The methyl deformation modes mainly coupled with the in-plane bending vibrations. The bands obtained at 1020 and 651 cm^{-1} in IR and Raman spectrum of PYRPCA and at 1028 and 654 cm^{-1} in the IR and Raman spectrum of PYRPCN were assigned to CH_3 in-plane and out-of-plane rocking modes. The band at 399 cm^{-1} in the IR spectrum of PYRPCA and at 404 cm^{-1} in the IR spectrum of PYRPCN is attributed to the methyl twisting mode.

Pyrazole–pyridine ring vibrations

Many ring modes are affected by substitutions to pyrazole and pyridine rings. The pyridine ring absorb strongly in the region 1630–1300 cm^{-1} .³⁶ In the present study, for the PYRPCA molecule, the peaks absorbing at 1614, 1562, 1530, 1497 and 1372 cm^{-1} in the IR spectrum and at 1623, 1563, 1525, 1493 and 1362 cm^{-1} in the Raman spectrum (*cf.* Table V-SM) were assigned to ring stretching vibrations. For PYRPCN, peaks absorbing at 1616, 1595, 1536, 1481 and 1308 cm^{-1} in the IR spectrum and at 1605, 1592, 1535, 1479 and 1304 cm^{-1} in the Raman spectrum were assigned to the pyridine ring. The pyrazole ring has several bands of variable intensities in the range of 1530–1013 cm^{-1} due to ring stretching vibrations.³⁷ In the present study, the IR peaks observed at 1429, 1342, 1237 and 1060 cm^{-1} and the Raman bands at 1419, 1342, 1232 and 1057 cm^{-1} were assigned to ring stretching vibrations. Pyrazole ring deformations were observed at 1016, 694, 515 and 487 cm^{-1} and the pyridine ring deformation vibrations at 900, 674, 515 and 487 cm^{-1} . These bands are also observed at the same wave number in the IR and Raman spectra of the PYRPCN molecule. For most of the remaining ring vibrations, the overall agreement was satisfactory. Small changes in frequencies observed for these modes are due to changes in the force constant/reduced mass ratio, resulting mainly due to the extent of mixing between the rings and substituent group vibrations.³⁸

CONCLUSIONS

Presently, the DFT-based SQM approach provides the most reliable information on the vibrational properties of large-size molecules. This method, using the Pulay standard scale factors, performed well for pyrazolo-pyridine derivatives.

Based on the SQM force field, complete vibrational analyses of the title compounds were performed, resulting in the assignment of all the fundamentals. The overall good quality of the SQM force field was confirmed by the achieved root mean square deviation of 13.9 and 10.12 cm^{-1} between the experimental and scale frequencies for PYRPCA and PYRPCN, respectively. The assignment of most of the fundamentals provided in the present study is unambiguous taking advantage of selective scaling (correcting effectively the different systematic errors of the computed force field) and the fairly good information on the IR and Raman intensities from the density functional theory. It is remarkable that all the vibrations affected by the strong hydrogen bonding were described satisfactorily by the scaled DFT force field with modification of the original scale factors of C=O, NH, C≡N and NH₂ stretching and bending. From the view of an extension of the Pulay DFT-based SQM method for the strongly hydrogen-bonded systems, the above results are very promising. Vibrations of the OH and CO and NH₂ and NH groups reflect the effect of the strong inter-molecular hydrogen bonding. In addition, the intermolecular hydrogen bonding interaction strengthens the conjugation of the NH₂ and COOH groups with the pyrazolo-pyridine rings.

SUPPLEMENTARY MATERIAL

TABLE V-SM: Comparison of the observed and calculated frequencies (in cm^{-1}) of the fundamental vibrations of 6-amino-3-methyl-1-phenyl-1*H*-pyrazolo[3,4-*b*]pyridine-5-carboxylic acid (PYRPCA) and 6,7-dihydro-3-methyl-6-oxo-1-phenyl-1*H*-pyrazolo[3,4-*b*]pyridine-5-carbonitrile (PYRPCN) obtained by DFT force fields by B3LYP/6-31G*, is available electronically from <http://www.shd.org.rs/JSCS> or from the corresponding author on request.

ИЗВОД

ТЕОРИЈСКА И ЕКСПЕРИМЕНТАЛНА ИСТРАЖИВАЊА СТРУКТУРЕ И ВИБРАЦИОНИХ СПЕКТРА 6-АМИНО-3-МЕТИЛ-1-ФЕНИЛ-1*H*-ПИРАЗОЛО[3,4-*b*]ПИРИДИН-5-КАРБОКСИЛНЕ КИСЕЛИНЕ И 6,7-ДИХИДРО-3-МЕТИЛ-6-ОКСО-1-ФЕНИЛ-1*H*-ПИРАЗОЛО[3,4-*b*]ПИРИДИН-5-КАРБОНИТРИЛА

KHALED BAHGAT¹, NAZM AL-DEN JASEM² и TALAAT EL-EMARY³

¹Chemistry Department, Faculty of Petroleum and Mining Engineering, Suez Canal University, Suez, Egypt,

²Chemistry Department, Faculty of Sciences, Aleppo University, Syria и ³Chemistry Department, Faculty of Science, Assiut University, Assiut, Egypt

FT-IR и FT-рамански спектри чврсте фазе 6-амино-3-метил-1-фенил-1*H*-пиразоло[3,4-*b*]пиридин-5-карбоксилне киселине (PYRPCA) и 6,7-дихидро-3-метил-6-оксо-1-фенил-1*H*-пиразоло[3,4-*b*]пиридин-5-карбонитрила (PYRPCN) снимљени су у области 4000–400 cm^{-1} . Спектри су тумачени помоћу нормалне координатне анализе, праћене потпуном оптимизацијом структуре и прорачуном поља сила, који су засновани на функционалној теорији густине (DFT) уз коришћење стандардних метода B3LYP, BLYP и *ab initio* RHF, заснованих на 6-31G* поставци, уз одређивање размере помоћу предложеног скупа размерних фактора, чиме се добило задовољавајуће слагање између уочених и израчунатих учестаности. На основу овога, постављено је прилагођено квантно-механичко поље сила (SQM) као поуздан темељни опис PYRPCA и PYRPCN. Израчунавања су предвидела преовлађивање различитих таутомера за PYRPCA

и кето-енолних таутомера за PYRPCN. Формирање међумолекулских водоничних веза доводи до најстабилније конформације PYRPCA. Карактеристика овог водоничног повезивања јесте ефекат јачања у односу на коњугацију NH₂ и COOH група са пиридинским прстеном.

(Примљено 22. октобра 2008, ревидирано 12. фебруара 2009)

REFERENCES

1. B. A. Hess Jr., J. Schaad, P. Carsky, R. Zahradnik, *Chem. Rev.* **86** (1986) 709
2. P. Pulay, X. Zhou, G. Fogarasi, in NATOASI Series, Vol.C406, R. Fausto, Ed., Kluwer, Dordrecht, 1993, p. p. 99–112
3. C. E. Blom, C. Altona, *Mol. Phys.* **31** (1976) 1377
4. P. Pulay, G. Fogarasi, G. Pongor, J. E. Boggs, A. Vargha, *J. Am. Chem. Soc.* **105** (1983) 7037
5. G. Fogarasi, P. Pulay, in *Vibrational Spectra and Structure*, Vol. 14, J. R. Durig, Ed., Elsevier, Amsterdam, 1985, p. 125
6. G. Fogarasi, *Spectrochim. Acta* **52A** (1997) 1211
7. G. Pongor, P. Pulay, G. Fogarasi, J. E. Boggs, *J. Am. Chem. Soc.* **106** (1984) 2765
8. G. Rauhut, P. Pulay, *J. Phys. Chem.* **99** (1995) 3093
9. G. Rauhut, P. Pulay, *J. Am. Chem. Soc.* **117** (1995) 4167
10. P. M. Kozlowski, G. Rauhut, P. Pulay, *J. Chem. Phys.* **103** (1995) 5650
11. A. Kovacs, K. B. Borisenko, G. Pongor, *Chem. Phys. Lett.* **280** (1997) 343
12. I. Macsari, V. Izvekov, A. Kovacs, *Chem. Phys. Lett.* **269** (1997) 343
13. B. M. Lynch, M. A. Teo, H. C. Pedrotti, *Can. J. Chem.* **66** (1988) 420
14. M. Makowska-Janusik, I. V. Kityk, *Spectrochim. Acta A* **65** (2006) 511
15. A. M. Hussein, T. I. El-Emary, *J. Chem. Res., Synop. 1* (1998) 241
16. J. Haufel, E. Breitmaier, *Angew. Chem. Int. Ed.* **13** (1974) 604
17. M. J. Frisch, G. W. Trucks, H. B. Schlegel, P. M. Johnson, M. A. Robb, J. R. Cheeseman, T. A. Keith, G. A. Peterson, J. A. Montgomery, M. A. Al-Laham, U. G. Zakrzewski, J. V. Ortiz, J. B. Foresman, C. Y. Reng, P. Y. Ayala, M. W. Wong, J. L. Andres, E. S. Replogle, R. Gomperts, R. L. Martin, D. J. Fox, J. S. Binkley, D. J. Defrees, J. Baker, J. P. Stewart, M. Head-Gordon, C. Gonzalez, A. Pople, gaussian94w (revision B. 3), Gaussian, Inc., Pittsburgh, PA, 1995
18. A. D. Becke, *J. Chem. Phys.* **98** (1993) 5648
19. C. Lee, W. Yang, R. G. Parr, *Phys. Rev. B* **37** (1998) 785
20. G. Fogarasi, X. Zhou, P. W. Taylor, P. Pulay, *J. Am. Chem. Soc.* **114** (1992) 8191
21. T. Sundius, *J. Mol. Struct.* **218** (1990) 321
22. T. Sundius, *Vib. Spectrosc.* **29** (2002) 89
23. Molvib (V. 7.0), Calculation of Harmonic Force Fields and Vibrational Modes of Molecules, QCPE Program No. 807, 2002
24. F. A. Cotton, *Chemical Application of Group Theory*, Wiley Interscience, New York, 1971
25. A. J. Dobson, R. E. Gerkin, *Acta Crystallogr. C* **53** (1997) 1427
26. K. B. Borisenko, C. W. Bock, I. Hargittai, *J. Phys. Chem.* **98** (1994) 1442
27. N. Z. Tugusheva, L. M. Alekseeva, A. S. Shashkov, V. V. Chernyshev, V. G. Granik, *Russ. Chem. Bull., Int. Ed.* **55** (2006) 1475
28. G. Varsanyi, *Assignments for Vibrational Spectra of 700 Benzene Derivatives*, Vols. 1 and 2, Adam Hilger, London, 1974

29. V. K. Rastogi, M. P. Rajpoot, S. N. Sharma, *Indian J. Phys.* **58B** (1984) 311
30. V. Chis, *Chem. Phys.* **300** (2004) 1
31. G. C. Pimentel, A. L. McClellan, *The Hydrogen Bond*, W. H. Freeman, San Francisco, CA, 1960
32. A. Szab, A. Kovács, *J. Mol. Struct.* **510** (1999) 215
33. A. Kovács, V. Izvekov, G. Keresztury, G. Pongor, *Chem. Phys.* **238** (1998) 231
34. G. Socrates, *Infrared and Raman Characteristic Group Frequencies, Tables and Charts*, 3rd ed., Wiley, Chichester, 2001
35. V. Krishnakumar, V. Balachandran, *Spectrochim. Acta A* **61** (2005) 2510
36. A. Topaçli, S. Bayari, *Spectrochim. Acta A* **57** (2001) 1385
37. M. Majoube, *J. Raman Spectrosc.* **20** (1989) 2434
38. F. Billes, H. Endrédi, G. Jalsovszky, *THEOCHEM* **465** (1999) 157.